

Constructing atomic layer g-C₃N₄/CdS nanoheterojunction with efficiently enhanced visible light photocatalytic activity

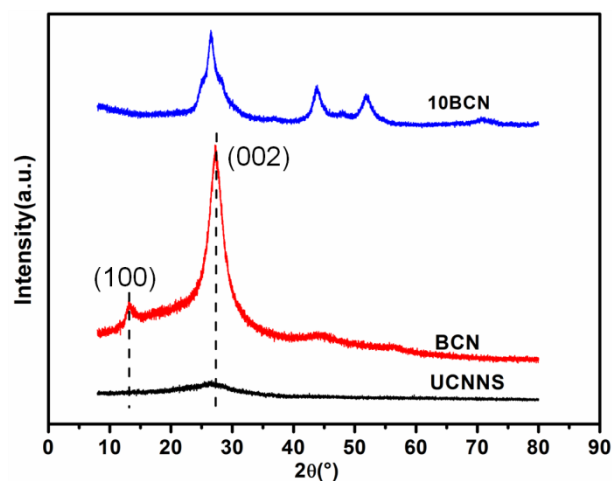


Figure S1. XRD patterns of BCN, UCNNS, and Bulk 10CN

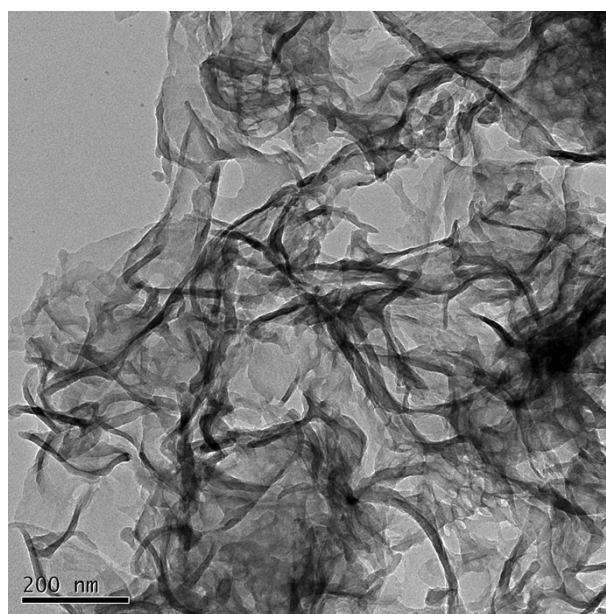


Figure S2. TEM image of UCNNS

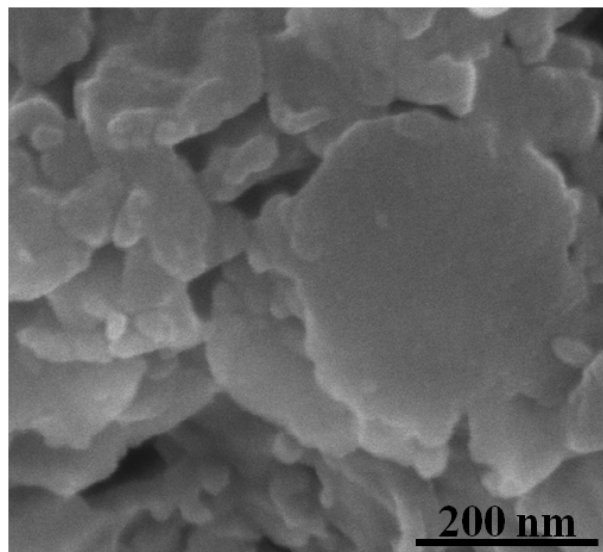


Figure S3. SEM image of bulk g-C₃N₄ (BCN)

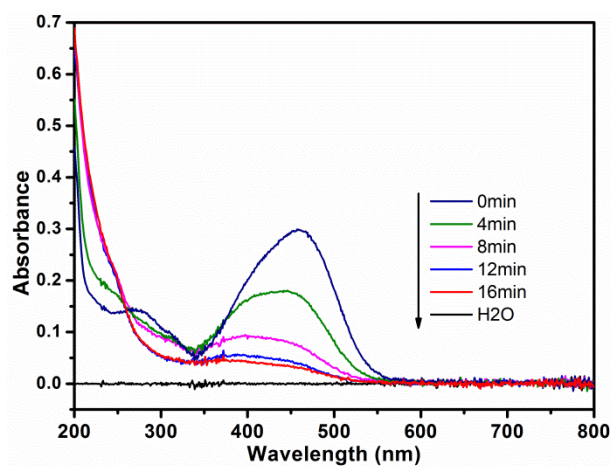


Figure S4. Temporal UV-visible absorption spectral changes for the MO solution (5 mg/L) with 10CN sample under visible light irradiation ($\lambda \geq 420$ nm)

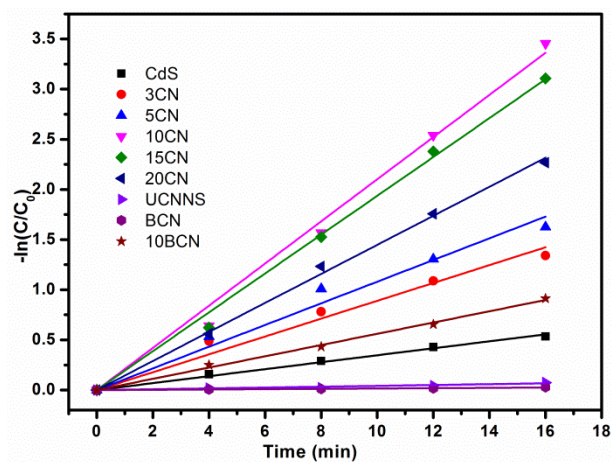


Figure S5. The photodegrade rate of MO using pseudo-first-order reaction kinetics

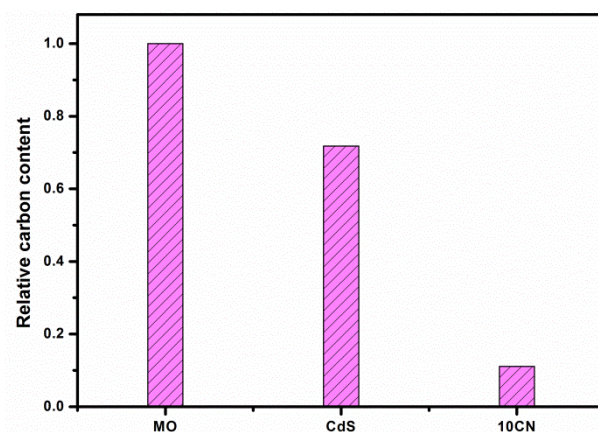


Figure S6. The TOC for CdS and 10CN sample after visible light irradiation

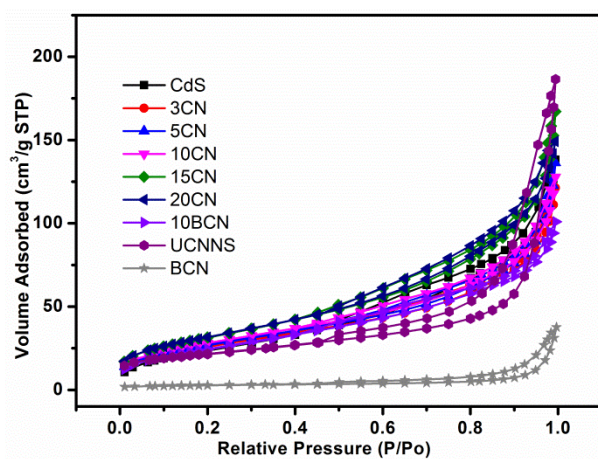


Figure S7. Nitrogen adsorption-desorption isotherms for as-prepared samples.

Table S1. The physical properties of the samples

Sample	CdS	3CN	5CN	10 CN	15 CN	20 CN	UCN NS	BCN	10 BCN
S_{BET} (m^2/g)	91.3	97.1	101.0	104.3	116.6	116.0	76.5	9.4	91.9
Pore volume (cm^3/g)	0.21	0.19	0.21	0.26	0.22	0.23	0.29	0.06	0.16

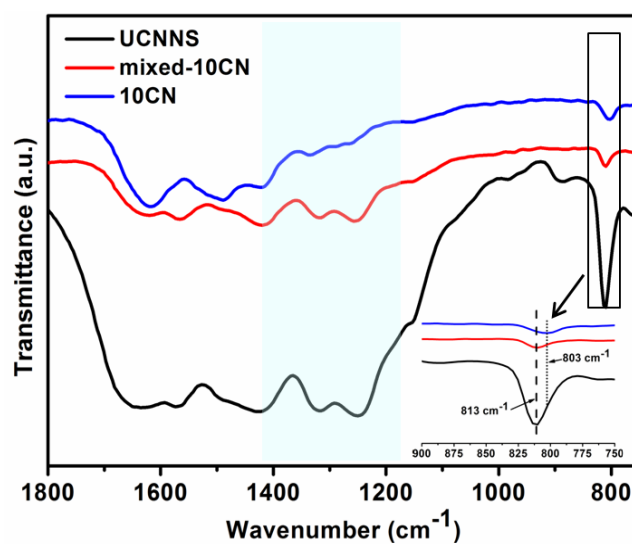


Figure S8. Comparison of FTIR spectra for UCNNS, mixed-10CN, and 10CN.

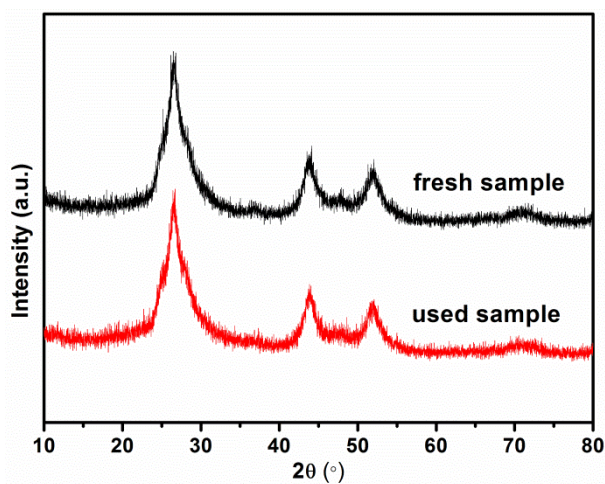


Figure S9. XRD patterns of as-prepared 10CN sample and the sample after it was used in cycling photocatalytic degradation test.

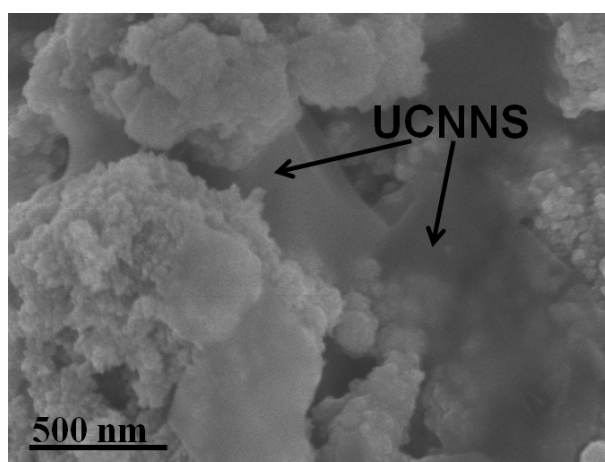


Figure S10. SEM of as-prepared 10CN sample after it was used in cycling photocatalytic degradation test.

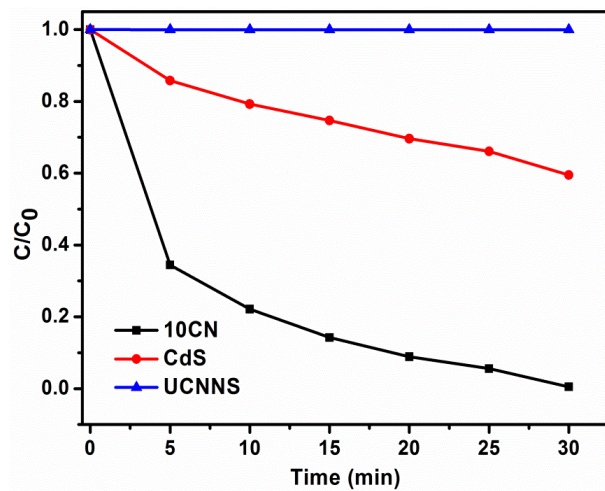


Figure S11. Photocatalytic degradation of MO over the 10CN, CdS, and UCNNS samples under visible light with a band-selective filter (450 ± 15 nm).

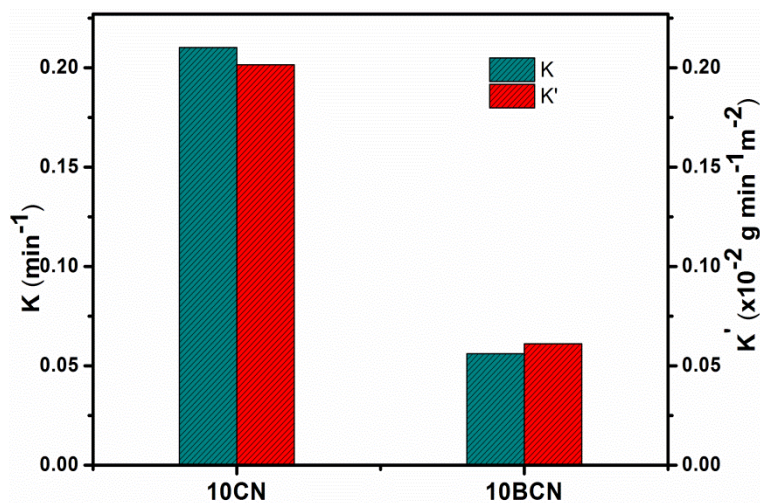


Figure S12. The comparison of reaction rate constants for photocatalytic degradation of MO over samples over 10CN and 10BCN before and after normalization with surface area.